

**An-Najah National University
Faculty of Graduate Studies**

**Heat Capacity of Two Electrons
Quantum Dot in an External Magnetic
Field by Variational Method**

**By
Ayham Anwar Shaer**

**Supervisor
Prof. Mohammad Elsaid**

**Co-supervisor
Dr. Musa Elhasan**

**This Thesis is Submitted in Partial Fulfillment of the
Requirements for the Degree of Master of Physics, Faculty of
Graduate Studies, An-Najah National University, Nablus,
Palestine.**

2015

**Heat Capacity of Two Electrons
Quantum Dot in an External Magnetic
Field by Variational Method**

**By
Ayham Anwar Shaer**

This thesis was defended successfully on 12/8/2015 and approved by:

Defense Committee Members

Signature

Prof. Mohammad Elsaid (Supervisor).

..... M. Khalil

Dr. Musa Elhasan (Co-Supervisor).

.....

Dr. Hussein Shanak (External examiner).

.....

Dr. Khaled Haiwi (Internal examiner).

.....

III

Dedication

For my family for their love and support

Acknowledgments

I would like to express my sincere thanks to my supervisor and instructor Prof. Mohammed Elsaid for his guidance, assistance, supervision and contribution of valuable suggestions. And I would like to thank Dr. Musa Elhasan for his efforts and time. I can't forget to thank Dr. Khalid Ilaiwi for his first touch in Mathematica program. Finally I would like to thank all friends for providing encouragement and support.

الإقرار

أنا الموقع أدناه مقدم الأطروحة التي تحمل عنوان

**Heat Capacity of Two Electrons
Quantum Dot in an External Magnetic
Field by Variational Method**

السعة الحرارية لنقطة كمية تحتوي إلكترونين
في مجال مغناطيسي خارجي "بطريقة المتغيرات"

أقر بأن ما اشتملت عليه هذه الرسالة إنما هو نتاج جهدي الخاص، باستثناء ما تمت الإشارة إليه حيثما ورد، وأن هذه الرسالة ككل أو جزء منها لم يقدم من قبل لنيل أية درجة أو بحث علمي أو بحثي لدى أية مؤسسة تعليمية أو بحثية أخرى

Declaration

The work provided in this thesis, unless otherwise referenced, is the researcher's own work, and has not been submitted elsewhere for any other degree or qualification.

Student's name: Ayham Anwar Shaer : اسم الطالب

Signature: *Ayham Shaer* : التوقيع

Date: *12/8/2015* : التاريخ

Table of Contents

No.	Content	Page
	Dedication	III
	Acknowledgement	IV
	Declaration	V
	Table of Contents	VI
	List of Tables	VII
	List of Figures	VIII
	List of Symbols and Abbreviations	X
	Abstract	XII
	Chapter One: Introduction	1
1.1	Low Dimensional Crystal	2
1.2	Literature Survey	4
1.3	Heterostructure and confinement potential	8
1.4	Objectives	11
1.5	Thesis Layout	12
	Chapter Two: Theory	13
2.1	Quantum Dot Hamiltonian	14
2.2	Variation of Parameter Method	19
2.3	Heat Capacity	24
	Chapter Three	25
3.1	Quantum Dot Spectra	26
3.2	Heat Capacity	32
	Chapter Four: Conclusion and Future Work	36
	References	38

List of Tables

No.	Table Captions	Page
Table (3.1)	The relative motion energy spectrum of the QD states ($m=0,1,2,\dots,8$) against the magnetic field for two interacting electrons for $\omega_0 = \frac{2}{3} R^*$ (the underlined energy values show the angular momentum transitions of the ground state of the QD)	29
Table (3.2)	The heat capacity of two interacting electrons in the QD against the temperature for $\omega_0 = \frac{2}{3} R^*$ and $\frac{\omega_c}{\omega_0} = 0.5$	34

List of Figures

No.	Figure Captions	Page
Figure (1.1)	Schematic image and the density of state as function of energy for various confinement systems: bulk (3D) , quantum well (2D), quantum wire (1D), and quantum dot (0D).	3
Figure (1.2)	The source-drain current against the gate voltage for vertical QD.	5
Figure (1.3)	The single-electron capacitance spectroscopy as function of magnetic field for a QD with various electron numbers.	6
Figure (1.4)	Schematic picture of a three-terminal QD.	6
Figure (1.5)	Scanning tunneling microscope images for single QDs fabricated from GaAs/AlGaAs and charged with few electrons.	9
Figure (1.6)	Schematic picture for the mechanism of confining electrons in semiconductor QD heterostructure a) 2DEG at the interface between GaAs and AlGaAs heterostructure. The electrons in the 2DEG is due to the ionization of silicon donors located in the n-AlGaAs layer. b) The metal electrodes on the surface of heterostructure are used to apply a negative voltage in order to deplete locally the electrons below 2DEG. In this way, we can confine the electrons in zero dimensions to obtain a QD system.	10
Figure (1.7)	Negative gate potentials used to confine the electrons in a double quantum dot (DQD).	11
Figure (3.1)	The energy spectra of Fock-Darwin states and the corresponding degeneracy.	26
Figure (3.2)	The dependence of the relative motion energy spectra on the magnetic field for two non-interacting electrons in a QD at confining frequency $\frac{\omega_0}{\omega_c} = \frac{2}{3} R^*$	27
Figure (3.3)	The computed relative motion energy spectra of two interacting electrons quantum dot against the strength of the magnetic field for $\omega_0 = \frac{2}{3} R^*$, and angular momentum $m^r = 0, \pm 1, \pm 2, \pm 3$.	28

No.	Figure Captions	Page
Figure (3.4)	The singlet-triplet energy level diagram of the QD. Confining frequency ω_c against the strength of the magnetic field ω_o .	31
Figure (3.5)	The exchange energy of the two interacting electrons in a QD against the magnetic field strength for $\omega_o = \frac{2}{3} R^*$.	32
Figure (3.6)	The dependence of the heat capacity on the temperature for fixed value of magnetic field $\omega_c = 0.5 R^*$ and various confinement frequencies: $\omega_o = \frac{2}{3} R^*$ Solid, $\omega_o = 0.6 R^*$ Dashed.	33
Figure (3.7)	The heat capacity as function of magnetic field strength for fixed value of temperature ($T = 0.1$ K) and confinement frequency $\omega_o = \frac{2}{3} R^*$.	35

List of Symbols and Abbreviations

QD	Quantum dot
3D	Three dimension
2D	Two dimension
1D	One dimension
0D	Zero dimension (quantum dot)
\mathcal{M}	Magnetization
C_V	Heat capacity
I	Current
A	Ampere
pA	Pico Ampere
Sin	Spin Singlet state
Tri	Spin Triplet state
Sin-Tri	Singlet-triplet transition
V_{SD}	Source-Drain voltage
V_G	Gate voltage
ω_c	Confining frequency
ω_c	Cyclotron frequency
B	Magnetic field
χ	Magnetic susceptibility
GaAs	Gallium Arsenide
AlGaAs	Aluminum Gallium Arsenide
MBE	Molecular beam epitaxy
n- AlGaAs	Negative type Aluminum Gallium Arsenide
2DEG	Two dimensional electron gas
$V(x,y)$	Lateral confinement potential
e	Charge of electron
m	Mass of electron
m^*	Effective mass of electron
$\hbar p$	The linear momentum
R	Center of mass position
r	Relative motion position
A(r)	Vector potential
c	Speed of light
ϵ	The dielectric constant of material
R^*	Effective Rydberg unit
\hbar	Reduced Blank's constant
ω	Effective frequency
∇	Gradient operator

XI

i	Imaginary number
ψ	Wave function
K	Kelvin Degree
T	Temperature
n	Principle quantum number
m	Angular quantum number
S	Spin

XII

**Heat Capacity of Two Electrons
Quantum Dot in an External Magnetic
Field by Variational Method**

By

Ayham Anwar Shaer

Supervisor

Prof. Mohammad Elsaid

Co-supervisor

Dr. Musa Elhasan

Abstract

The heat capacity of two interacting electrons confined in a quantum dot presented in a magnetic field had been calculated by solving the Hamiltonian using variational method. We had investigated the dependence of the heat capacity on temperature, magnetic field and confining frequency. The singlet triplet transition in the ground state of the quantum dot spectra and the corresponding jumps in the heat capacity curves had been shown. The comparisons show that our results are in very good agreement with reported works.

Chapter One

Introduction

1.1 Low Dimensional Crystal

1.2 Literature Survey

1.3 Heterostructure and confinement potential

1.4 Objectives

1.5 Thesis Layout

Chapter One

Introduction

1.1 Low dimensional crystal

Low dimensional systems such as quantum dots, quantum wires and quantum wells are semiconductors whose size confine the electrons in a limited size (few nanometers) in three, two and one dimension respectively. The confinement phenomena change significantly the density of state of the system and the energy spectra. For quantum dot (zero dimensional system) the density of state shows a discrete behavior unlike to the other confinements which have a continuous density of state, and means a fully quantized energy levels due to its three dimensional confinement. The density of state for these confinements are shown in Figure (1.1).

The nanofabrication techniques allow us to control precisely both the size and the shape of the low dimensional system. The electronic characteristics of a quantum dot (QD) depend strongly on the size and shape, and this unique parameter effects are impossible for bulk system. The diameter of the QDs is about 100 nm.

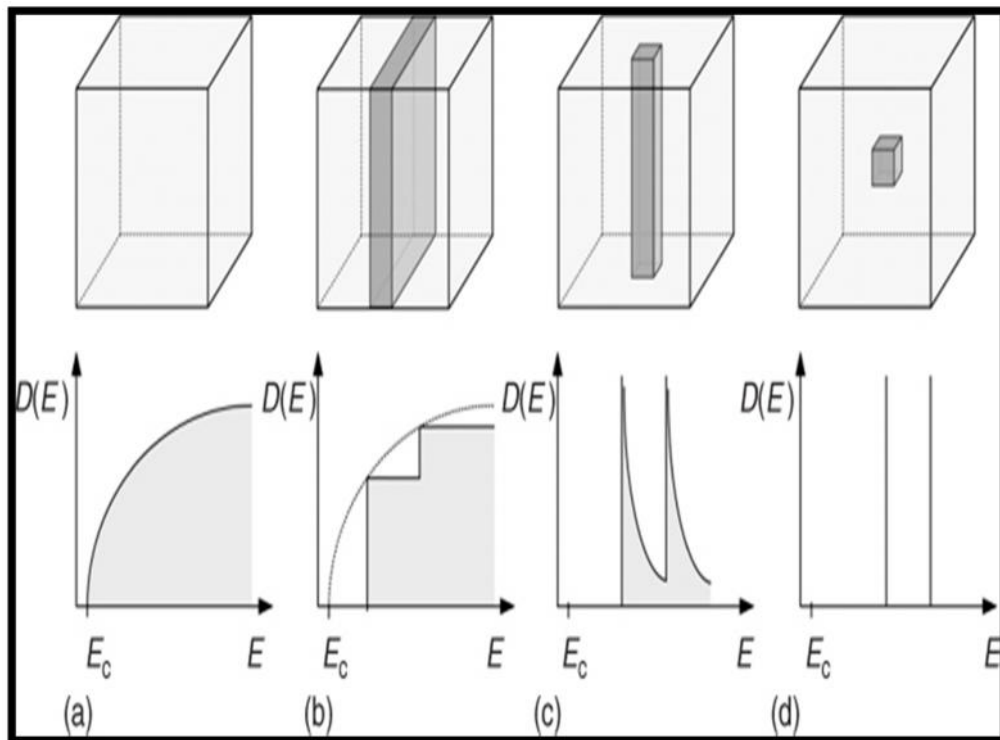


Figure (1.1) Schematic image and the density of state as function of energy for various confinement systems: bulk (3D) , quantum well (2D), quantum wire (1D), and quantum dot (0D).

QDs, or artificial atoms, had been the subject of interest research due to its physical properties and great potential device applications such as quantum dot lasers, solar cells, single electron transistors and quantum computers [1- 6]. The application of a magnetic field perpendicular to the dot plane will introduce an additional structure on the energy levels and on the correlation effects of the interacting electrons confined in a quantum dot.

In early 1980s, the first QD were successfully made in laboratory, this forced to investigate the properties of the quantum dot system and to study the effect of the size, material, and shape.

The QDs can be fabricated by two different ways, the first one is made by using lithography techniques of microchip manufacturing; and the second approach can be done by applying chemical processes to get a QD from bulk material.

1.2 Literature survey

The electronic properties of the quantum dots depend strongly on the interplay between electron-electron interaction (coulomb energy), confining potential, and the applied magnetic field. The existence of coulomb and parabolic potential makes the exact analytical solution of the quantum dot's Hamiltonian not possible.

Different theoretical methods had been used to solve the two electrons in a quantum dot Hamiltonian, to obtain the eigenenergies and eigenstates [7-23].

Maksym and Chakraborty [7] had used the diagonalization method to obtain the eigenenergies of interacting electrons in a magnetic field and show the transitions in the angular momentum of the ground state. They had also calculated the heat capacity curve for both interacting and non-interacting confined electrons in the QD presented in a magnetic field. The interacting model shows very different behavior from non-interacting electrons, and the oscillations in these thermodynamic quantities like magnetization (\mathcal{M}) and heat capacity (C_v) are attributed to the spin singlet-triplet transitions in the ground state energy of the quantum dot. This

transition had been shown as a peak in the current-voltage curve as displayed in figure (1.2). Wagner *et.al.*[8] had also studied this interesting QD system and predicted the oscillations between spin-singlet (Sin) and spin-triplet (Tri) ground state. This transition had been investigated experimentally by using single electron spectroscopy technique [9] for three terminal QD. This experimental energy eigenvalues curve had been presented in Ashoori work [2] figure (1.3), and a schematic picture of three terminal QD is presented in figure (1.4).

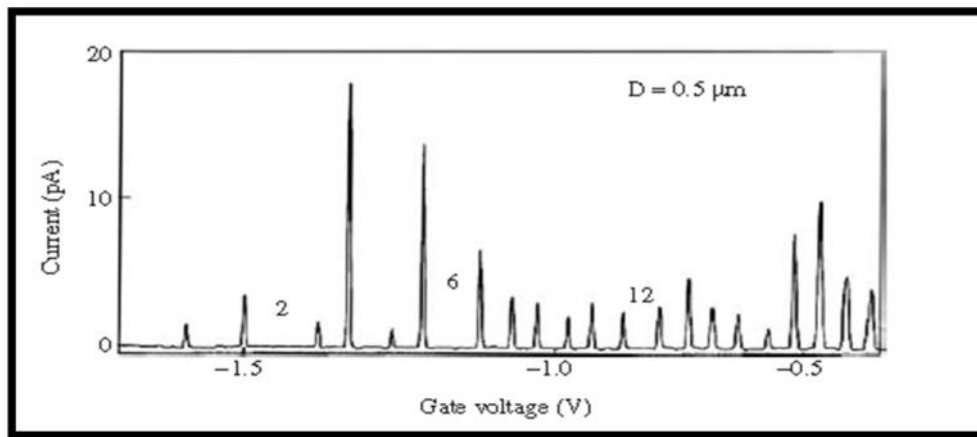


Figure (1.2) The source-drain current against the gate voltage for vertical QD.

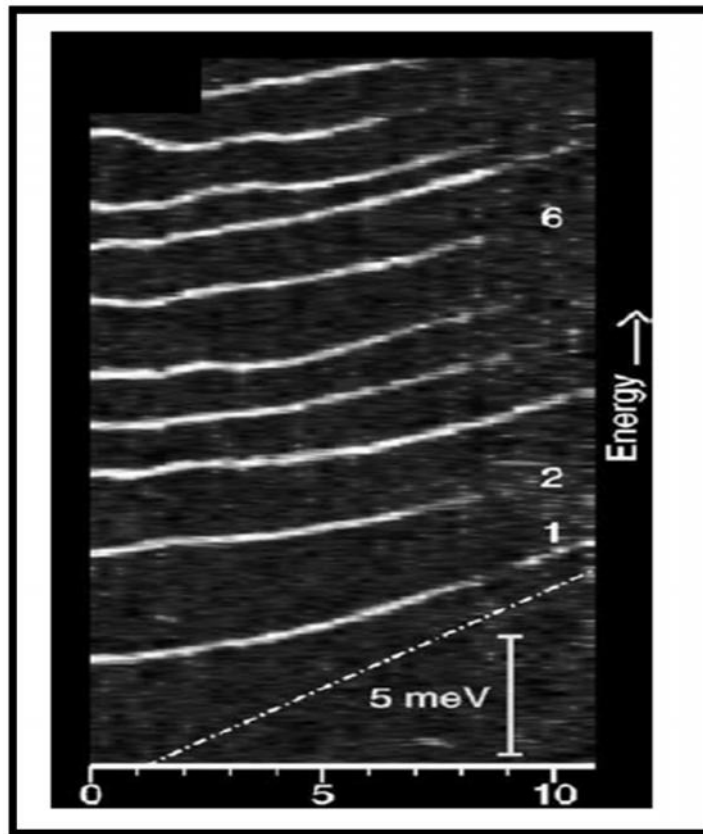


Figure (1.3) The single-electron capacitance spectroscopy as function of magnetic field for a QD with various electron numbers.

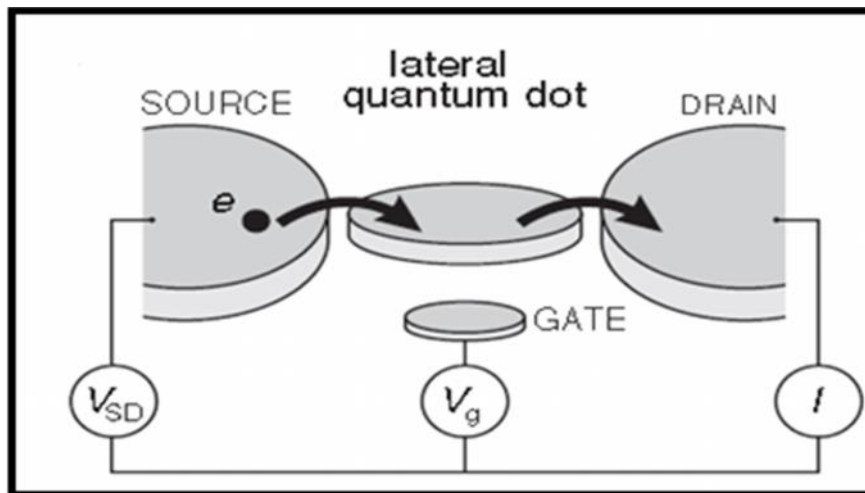


Figure (1.4) Schematic picture of a three-terminal QD.

Taut [10] had managed to obtain the exact analytical results for the energy spectrum of two interacting electrons through a coulomb potential, confined in a QD, just for particular values of the magnetic field strength.

In Refs. [11, 12] the authors had solved the QD-Hamiltonian by variational method and obtained the ground state energies for various values of magnetic field (μ_c), and confined frequency (ω_0). In addition, they had performed exact numerical diagonalization for the Helium QD-Hamiltonian and obtained the energy spectra for zero and finite magnetic field strength. Kandemir [13, 14] had found the closed form solution for this QD Hamiltonian and the corresponding eigenstates for particular values of the magnetic field strength and confinement frequencies. Elsaid *et.al.*[15-19] had used the dimensional expansion technique, in different works, to study and solve the QD-Hamiltonian and obtain the energies of the two interacting electrons for any arbitrary ratio of coulomb to confinement energies and gave an explanation to the level crossings. De Groote *et.al.*[20] had also calculated the magnetization, susceptibility and heat capacity of helium like confined QDs and obtained the additional structure in the heat capacity. In a detailed study, Nguyen and Peeters [21] had considered the QD helium in the presence of a single magnetic ion and applied magnetic field taking into account the electron-electron correlation in many quantum dots. They had shown the dependence of these thermal and magnetic quantities: C_v , \mathcal{M} and χ on the strength of the magnetic field, confinement frequency, magnetic ion position and temperature. They had observed that the crossings in the energy levels show up as peaks in the heat capacity and magnetization.

Very recently, Boyacioglu and Chatterjee [22] had studied the behavior of heat capacity of a single quantum dot confined with a Gaussian potential model. They had observed that the heat capacity curve shows peaks structure at low temperature. Helle *et.al.* [23] had computed the magnetization of a rectangular QD in a high magnetic field and the results show the oscillation and smooth behavior in the magnetization curve for both, interacting and non-interacting confined electrons, respectively.

1.3 Hetrostructure and confinement potential

The nanofabrication methods allow to the researchers fabricate electronic structures where the electrons are confined in a small regions of the order of nanometers (QDs). The QD is a small island on a semiconductor heterostructure, where the shape of the QD and the number of the electrons can be controlled by an external voltage. A scanning tunneling microscope image is shown in figure (1.5) for double quantum dot (DQD) which had been charged with few electrons, in this case the QD

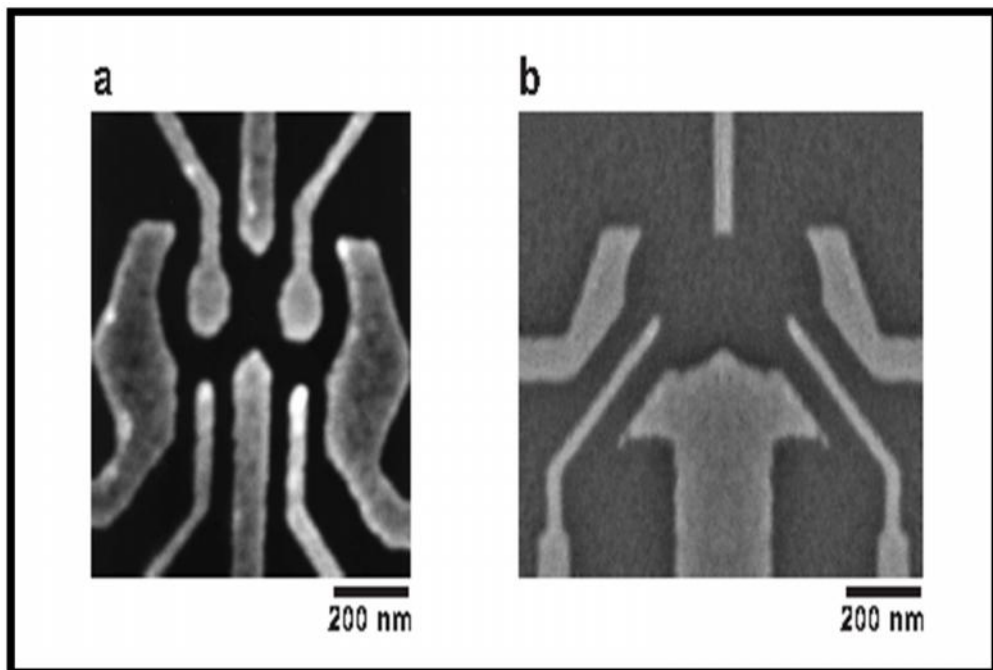


Figure (1.5) Scanning tunneling microscope images for single QDs fabricated from GaAs/AlGaAs and charged with few electrons.

is made from GaAs/AlGaAs semiconductor heterostructure. The heterostructure is growing by using the molecular beam epitaxy (MBE) method.

The AlGaAs layer is doped with Silicon donors in order to have free electrons in the heterostructure (n type AlGaAs). These free electrons move from AlGaAs layer with high band gap to GaAs layer with lower band gap. The electrons are trapped in the quantum well of GaAs layer. In this way we create a 2D structure where the motion of the electrons is quantized along the growth axis (z direction) while the electron is free to move in xy plane Fig (1.6).

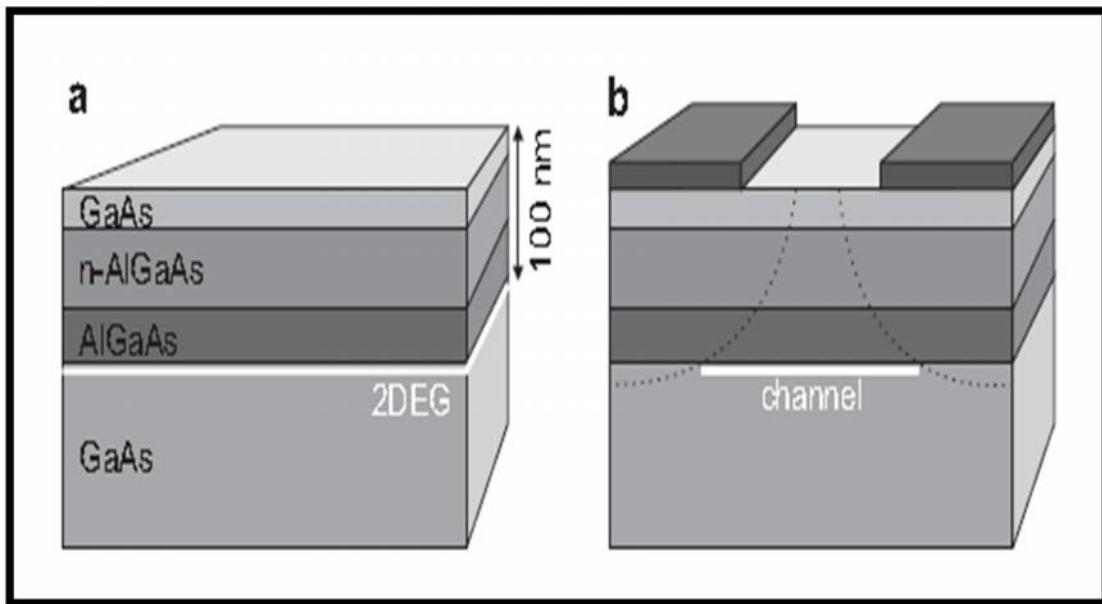


Figure (1.6) Schematic picture for the mechanism of confining electrons in semiconductor QD heterostructure a) 2DEG at the interface between GaAs and AlGaAs heterostructure. The electrons in the 2DEG is due to the ionization of silicon donors located in the n-AlGaAs layer. b) The metal electrodes on the surface of heterostructure are used to apply a negative voltage in order to deplete locally the electrons below 2DEG. In this way, we can confine the electrons in zero dimensions to obtain a QD system.

A negative voltage is finally applied on the surface of the heterostructure to reduce further the confinement region and creating one or more small islands from large two dimensional electron gas (2DEG) Fig (1.6 b) and Fig (1.7).

Lateral confinement potential $V(x, y)$ (due to the hetrostrucuture of the QD) quite similar to Coulomb potential which confined the electron in the real atom, and from here we can called the QD to be artificial atom. The lateral confinement potential is usually taken as a simple parabolic model, the theoretical-experimental comparisons show that harmonic oscillator model is the best to describe this confinement.

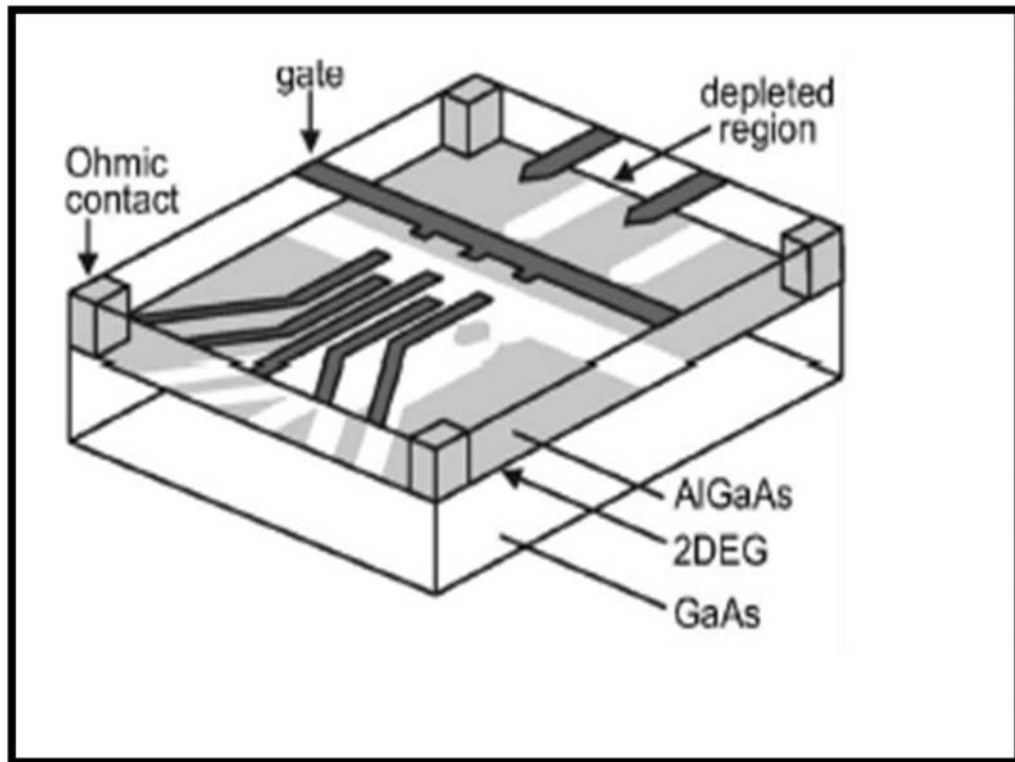


Figure (1.7) Negative gate potentials used to confine the electrons in a double quantum dot (DQD).

1.4 Objectives

This research project has two objectives which can be summarized as follows:

- To use variational method to reproduce the eigenenergies spectra of the two electrons quantum dot Hamiltonian for different ranges of magnetic field strength μ_c and confining potential μ_0 .
- The eigenenergies obtained above will be used to study the dependence of heat capacity of the quantum dot system on μ_c , μ_0 and temperature (T).

1.5 Outlines of thesis

In this work, the heat capacity has been calculated as a thermodynamic quantity for a quantum dot helium atom in which both the magnetic field and the electron-electron interaction are fully taken into account. Since, the eigenvalues of the electrons in the QD are the starting point to calculate the physical properties of the QD system. The variational method have been used to solve the QD Hamiltonian and obtain the eigenenergies. Second, the eigenenergies spectra had been calculated to display theoretically the behavior of heat capacity of the QD as a function of magnetic field strength, confining frequency and temperature.

The rest of this thesis is organized as follows: the Hamiltonian theory, the principle of the variation of parameter technique and how to calculate the heat capacity from the mean energy expression are presented in chapter II. In chapter III, the results of energy and heat capacity of our work had been displayed and discussed, while the final chapter devoted for conclusions and future work.

Chapter Two

Theory

2.1 Quantum Dot Hamiltonian

2.2 Variation of Parameter Method

2.3 Heat Capacity

Chapter Two

Theory

A detailed description for the theory of two electron quantum dot system and the method used will be given. The main three parts which consist the theory, namely: quantum dot Hamiltonian, variation of parameter method and the heat capacity will be presented in this chapter.

2.1 Quantum dot Hamiltonian

The effective mass Hamiltonian for two interacting electrons confined in a QD by a parabolic potential in a uniform magnetic field of strength B , applied along z direction is given by

$$H = \sum_{j=1}^2 \left\{ \frac{1}{2m^*} [\mathbf{p}(\mathbf{r}_j) + \frac{e}{c} \mathbf{A}(\mathbf{r}_j)]^2 + \frac{1}{2} m^* \omega_0^2 r_j^2 \right\} + \frac{-e^2}{\epsilon |\mathbf{r}_1 - \mathbf{r}_2|} \quad (2.1)$$

Where ω_0 is the confining frequency and ϵ is the dielectric constant \mathbf{r}_1 and \mathbf{r}_2 describe the positions of the first and second electron in the xy plane and the vector potential was taken to be:

$$\mathbf{A}(\mathbf{r}) = \frac{1}{2} \mathbf{B} \times \mathbf{r} \quad (2.2)$$

$$[\mathbf{A}, \mathbf{p}] = 0 \quad (2.3)$$

$$[\mathbf{A}, \mathbf{p}] = \frac{1}{2} \mathbf{B} \times \mathbf{r} \quad (2.4)$$

Expressing the Hamiltonian explicitly in terms of coordinates and momenta we get:

$$H = \frac{1}{2m} m \dot{r}_1^2 \omega_0^2 + \frac{1}{2m} m \dot{r}_2^2 \omega_0^2 + \frac{e_2}{\epsilon |r_2 - r_1|} + \frac{\left(p_1 + \frac{eA[r_1]}{c}\right)^2}{2m} + \frac{\left(p_2 + \frac{eA[r_2]}{c}\right)^2}{2m} \quad (2.5)$$

By using the standard coordinate transformation, The quantum dot Hamiltonian can be decoupled into center of mass (R) and relative (r) parts.

$$R = \frac{r_1 + r_2}{2} \quad (2.6)$$

$$r = r_2 - r_1 \quad (2.7)$$

$$P_R = p_1 + p_2 \quad (2.8)$$

$$P^R = \frac{p_1 + p_2}{2} \quad (2.9)$$

So the Hamiltonian can be written as

$$H = \frac{\left(\frac{eA[-\frac{r}{2} + R]}{c} - p_r + \frac{P_R}{2}\right)^2}{2m} + \frac{\left(\frac{eA[\frac{r}{2} + R]}{c} + p_r + \frac{P_R}{2}\right)^2}{2m} + \frac{1}{2}m\left(-\frac{r}{2} + R\right)^2 \omega_0^2 + \frac{1}{2}m\left(\frac{r}{2} + R\right)^2 \omega_0^2 + \frac{e^2}{r\epsilon} \quad (2.10)$$

The confining potential terms can be expressed as:

$$\frac{1}{2}m\left(-\frac{r}{2} + R\right)^2 \omega_0^2 + \frac{1}{2}m\left(\frac{r}{2} + R\right)^2 \omega_0^2 = \frac{1}{4}m r^2 \omega_0^2 + m R^2 \omega_0^2 \quad (2.11)$$

Using the linear property of the vector potential, we can separate kinetic energy terms into center of mass and relative part:

$$\begin{aligned} & \frac{\left(\frac{eA\left[-\frac{r}{2} + R\right]}{c} - p_r + \frac{P_R}{2} \right)^2}{2m} + \frac{\left(eA\left[\frac{r}{2} + R\right] + p_r + \frac{P_R}{2} \right)^2}{2m} \\ &= \frac{\left(\frac{eA[r]}{2c} + p_r \right)^2}{m} + \frac{\left(\frac{2eA[R]}{c} + P_R \right)^2}{4m} \end{aligned} \quad (2.12)$$

The full QD Hamiltonian in R, r coordinates has the following form:

$$\begin{aligned} H = & \frac{\left(\frac{eA[r]}{2c} + p_r \right)^2}{m} + \frac{\left(\frac{2eA[R]}{c} + P_R \right)^2}{4m} + \frac{1}{4} m r^2 \\ & + m R^2 + \frac{e^2}{\epsilon r} \end{aligned} \quad (2.13)$$

Finally, the complete two electron QD Hamiltonian is separated into center of mass Hamiltonian H_{CM} and relative Hamiltonian Part H_r as shown below:

$$H = H_{CM} + H_r \quad (2.14)$$

$$H_{CM} = \frac{1}{2M} \left[P_R + \frac{Q}{c} A(R) \right]^2 + \frac{1}{2} M \omega_0^2 R^2 \quad (2.15)$$

$$H_r = \frac{1}{2\mu} \left[p_r + \frac{q}{c} A(r) \right]^2 + \frac{1}{2} \mu \omega_0^2 r^2 + \frac{e^2}{\epsilon|r|} \quad (2.16)$$

Where M is the total mass = $2m$, Q is the total charge = $2e$, μ is reduce mass = $\frac{m}{2}$, and q is the reduce charge = $\frac{e}{2}$

The corresponding energy of this Hamiltonian equation (2.14) is:

$$E_{total} = E_{CM} + E_r \quad (2.17)$$

The center of mass Hamiltonian has The harmonic oscillator form which has well known fully analytical solution for wave function and energy that was found Independently by Fock [24] and Darwin [25] to be respectively:

$$\psi_{n,m}(R) = (-1)^n \frac{\beta^{|m+1|}}{\sqrt{\pi}} \left[\frac{n!}{(n+|m|)!} \right]^{\frac{1}{2}} e^{-\beta^2 R^2/2} R^{|m|} L_n^{|m|} \beta^2 R^2 e^{im\phi} \quad (2.18)$$

$$E_{n_{cm}, m_{cm}} = (2n_{cm} + |m_{cm}| + 1) \hbar \sqrt{\frac{\omega_c^2}{4} + \frac{z_0}{2}} + m_{cm} \frac{\hbar \omega_c}{2} \quad (2.19)$$

Where R and ϕ are the polar coordinates, n_{cm}, m_{cm} are the radial and azimuthal quantum numbers, respectively. And L_n^m is the associate laguerre polynomial, and $\beta = \sqrt{\frac{m\omega}{\hbar}}$, where $\omega = \sqrt{\frac{\omega_c^2}{4} + \frac{z_0}{2}}$

Due to existence of both coulomb and parabolic terms, The relative Hamiltonian part equation (2.16) does not have an analytical solution for all ranges of z_0 and ω_c , therefore, in this case we will use the variational method as an approximation method to find the energy spectra for the relative Hamiltonian in terms of a variational parameter.

By the help of a symmetric gauge , the relative Hamiltonian part can be written as:

$$H_r = \frac{1}{2\mu} \left(p_r^2 + \frac{q_2^2}{c^2} \frac{1}{4} B^2 r^2 + (-1) \frac{q}{c} \left(\frac{\partial}{\partial \phi} \right) \right) + \frac{1}{2} \mu \omega_0^2 r^2 + \frac{e^2}{\epsilon |r|} \quad (2.20)$$

Where the magnetic field is uniform with strength $\omega_c = \frac{eB}{cn}$ taken to be along z direction

$$\begin{aligned} \vec{L} \cdot \vec{B} &= L_z B \\ H_r &= \frac{p_r^2}{m} + \frac{1}{16} \omega_c^2 m r^2 + \frac{1}{2} \omega_c L_z + \frac{1}{4} m \omega_0^2 r^2 + \frac{e^2}{\epsilon |r|} \\ &= \frac{p_r^2}{m} + \frac{1}{4} m r^2 \left(\frac{\omega_c^2}{4} + \omega_0^2 \right) + \frac{1}{2} \omega_c L_z + \frac{e^2}{\epsilon |r|} \end{aligned} \quad (2.21)$$

The effective frequency is a sum of a nanostructure confining frequency and the magnetic field confining frequency, using a new parameter (α) defined as follow:

$$\alpha = \frac{1}{4} \sqrt{\omega_c^2 + \omega_0^2} \quad (2.22)$$

Now, The relative Hamiltonian is:

$$H_r = \frac{p_r^2}{m} + \frac{1}{4} m r^2 (\alpha^2) + \frac{1}{2} \omega_c L_z + \frac{e^2}{\epsilon |r|} \quad (2.23)$$

Which can be expressed in an operator form as:

$$\begin{aligned} H_r &= -\frac{\hbar^2}{m} \left(r^{-1/2} \frac{\partial^2}{\partial r^2} r^{1/2} + \frac{1}{r^2} \left(\frac{\partial^2}{\partial \phi^2} + \frac{1}{4} \right) \right) \\ &\quad + 4 m r^2 \alpha^2 - \frac{1}{2} i \hbar \frac{\partial}{\partial \phi} \omega_c + \frac{e^2}{\epsilon |r|} \end{aligned} \quad (2.24)$$

$$\quad (2.25)$$

Where

$$L_z = -i\hbar \frac{\partial}{\partial \phi} \tag{2.26}$$

$$= -i\hbar \frac{\partial}{\partial \phi} \tag{2.27}$$

$$\nabla^2 = \frac{1}{r^2} \frac{\partial}{\partial r} \left(r^2 \frac{\partial}{\partial r} \right) + \frac{1}{r^2} \left(\frac{\partial^2}{\partial \phi^2} + \dots \right) \tag{2.28}$$

2.2 Variation of parameter method

As we have mentioned early we will use the variational method as an approximation method to calculate the desired energy eigenvalues of the relative part Hamiltonian of the two electron quantum dot.

The principle idea for variational method that choosing the variational wave function with parameters C_i

$$\Psi = \sum C_i \psi_i(C_1, C_2, \dots, C_j) \tag{2.29}$$

and calculate the energy by solving Schrödinger equation

$$H \Psi = E \Psi \tag{2.30}$$

To find the energy in terms of the variational parameter, we should minimize the energy expression $E(C_1, C_2, \dots, C_j)$ with respect to each variational parameter C_i to reach a stable system:

$$\frac{\partial E(C_1, C_2, \dots, C_j)}{\partial C_i} = 0 \tag{2.31}$$

$$\frac{\partial^2 E((C_1, C_2, \dots, C_j))}{\partial C_i^2} > 0 \quad (2.32)$$

For $i = 1, 2, \dots$

In our problem, the adopted one parameter variational wave function is [26]:

$$\psi(r) = \frac{\sqrt[4]{\alpha} u_m(\rho) e^{im\phi}}{\sqrt{2\pi} \sqrt{\rho}} \quad (2.33)$$

Where

$$u_m(\rho) = \rho^{1/2+|m|} (1 + \beta\rho) e^{-\left(\frac{\rho^2}{2}\right)} \quad (2.34)$$

$$\rho = \sqrt{\frac{1 + \beta\rho}{\alpha}} r \quad (2.35)$$

We can write Schrödinger equation with complete relative Hamiltonian form and full variational wave function, in differential operator form, it takes the following picture:

$$\begin{aligned} & \left(-\frac{\hbar^2}{2m} \left(r^{-1/2} \frac{\partial^2}{\partial r^2} r^{1/2} + \frac{1}{r^2} \left(\frac{\partial^2}{\partial \phi^2} + \frac{1}{4} \right) \right) + 4mr^2 \alpha^2 \right. \\ & \left. - \frac{1}{2} i\hbar \frac{\partial}{\partial \phi} \left(\omega_c + \frac{e^2}{\epsilon|r|} \right) \right) \frac{\sqrt[4]{\alpha} u_m(\rho) e^{im\phi}}{\sqrt{2\pi} \sqrt{\rho}} \\ & = E_r \frac{\sqrt[4]{\alpha} u_m(\rho) e^{im\phi}}{\sqrt{2\pi} \sqrt{\rho}} \quad (2.36) \end{aligned}$$

Simplify the equation to be :

$$\left(-\frac{\hbar^2 e}{m} \left(\frac{\partial^2}{\partial r^2} + \frac{1}{r^2} \left(\frac{1}{4} - m \right) \right) + 4 m r^2 \alpha^2 - \frac{1}{2} \hbar m \omega_c + \frac{\epsilon^2}{\epsilon |r|} \right) u_m(\rho) = E_{\text{rm}} u_m(\rho) \quad (2.37)$$

In our calculations, we have used the following Atomic Rydberg units

$$e^2 = 2, \hbar = 1, m = 1, \epsilon = 1$$

Finally, the equation for a relative Hamiltonian coordinate part is

$$-2 \frac{d^2}{dr^2} + 2 \left(m^2 - \frac{1}{4} \right) \frac{1}{r^2} + \frac{5}{2} \omega_c m + \frac{2}{r^2} \alpha^2 + \frac{2}{r} \quad (2.38)$$

We have normalized our wave function

$$u_m(\rho) = C_m \rho^{1/2+|m|} \left(1 + \beta \rho \right) e^{-\left(\frac{\rho^2}{2} \right)} \quad (2.39)$$

Where β is the variational parameter, the normalizing constant is given as

$$C_m^2 = \frac{\sqrt{\alpha}}{(1 + \beta^2) \Gamma[1 + |m|] + \beta^2 |m| \Gamma[1 + |m|] + 2\beta \Gamma\left[\frac{3}{2} + |m|\right]} \quad (2.40)$$

The above normalization constant can be written in terms of a new constant

$$C_m^2 = \frac{\sqrt{\alpha}}{d + e\beta + f\beta^2} \quad (2.41)$$

Where

$$d = \frac{1}{2 \Gamma[1 + |m|]} \quad (2.41)$$

$$e = \Gamma\left[\frac{\beta}{2}\right] + |m| \Gamma\left[\frac{\beta}{2}\right] \quad (2.42)$$

$$f = \frac{1}{2 \Gamma[2 + |m|]} \quad (2.43)$$

We have found the energy spectra of the relative Hamiltonian part:

$$\begin{aligned} E^r = \frac{1}{2} \omega_c n^l + \frac{C_{2, \beta}^2 \alpha}{\sqrt{\alpha}} & \left(\frac{1}{2} n^l \Gamma[|m|] + \frac{1}{2} |m| \Gamma[|m|] + \frac{5}{8} \beta^2 |m| \Gamma[|m|] \right. \\ & + \frac{1}{2} m^2 \beta^2 \Gamma[|m|] + \frac{\Gamma\left[\frac{1}{2} + |m|\right]}{2\sqrt{\alpha}} - \frac{1}{4} \beta \Gamma\left[\frac{1}{2} + |m|\right] \\ & + m^2 \beta \Gamma\left[\frac{1}{2} + |m|\right] + \frac{\beta^2 \Gamma\left[\frac{1}{2} + |m|\right]}{4\sqrt{\alpha}} + \frac{\beta^2 |m| \Gamma\left[\frac{1}{2} + |m|\right]}{2\sqrt{\alpha}} \\ & + \frac{\beta \Gamma[1 + |m|]}{\sqrt{\alpha}} - \frac{1}{8} \beta^2 \Gamma[1 + |m|] + \frac{1}{2} m^2 \beta^2 \Gamma[1 + |m|] \\ & + \beta \Gamma\left[\frac{3}{2} + |m|\right] + \frac{1}{2} \Gamma[2 + |m|] + \beta^2 \Gamma[2 + |m|] \\ & \left. + \frac{1}{2} \beta^2 |m| \Gamma[2 + |m|] + \beta \Gamma\left[\frac{5}{2} + |m|\right] \right) \quad (2.44) \end{aligned}$$

Which can be written as

$$E^r(\beta) = -\frac{1}{2} m \omega_c + 2 \frac{\alpha}{\alpha} \frac{a + b\beta + c\beta}{d + e\beta + f\beta} \quad (2.45)$$

where

$$a = \frac{e}{(2|m| + 1)\sqrt{\alpha}} + 2f \quad (2.46)$$

$$b = \frac{2d}{\sqrt{\alpha}} + 2(|m| + 1)e \quad (2.47)$$

$$c = \frac{e}{2\sqrt{\alpha}} + (2|m|_z + 4|m| + 3)d \quad (2.48)$$

d, e, f which is previously defined in Equation (2.41-2.43) respectively.

The energy eigenvalues of H_r can be obtained by minimizing the energy expression equation (2.45) with respect to the variational parameter β namely

$$\frac{\partial E}{\partial \beta} = 0 \quad (2.49)$$

The value of the parameter β which satisfies the minimum energy requirement is

$$\beta_{\min} \rightarrow \frac{2}{\frac{cd - 2af - \sqrt{(2cd - 2af)^2 - 4(bd - ae)(ce - bf)}}{2(ce + bf)}} \quad (2.50)$$

So, the final energy expression in terms of the variational parameter value which satisfies the minimization condition is

$$E_r(\beta_{\min}) = -\frac{1}{2}m\omega_c + 2 \left\{ \frac{a + b\beta_{\min}}{d + e\beta_{\min}} + \frac{c\beta_{\min}^2}{f\beta_{\min}} \right\} \quad (2.51)$$

Having obtained the eigenenergies for the QD system for any state labeled by n, m quantum number, now we are able to calculate the exchange energy (J) define as the difference between the singlet (S=0, L is even) and triplet (S=1, L is odd) states:

$$J = E_{tri} - E_{sin} \quad (2.52)$$

For any range magnetic field and confining potential.

2.3 Heat capacity

The heat capacity C_v is defined as the amount of energy which is needed to increase the temperature of the system by one degree, and it is considered the most important thermal property.

To calculate the heat capacity of the two electron quantum dot system, first, we have evaluate the mean energy from the statistical energy expression [27]:

$$\langle E(T, B, \omega_o) \rangle = \frac{\sum_{\alpha=1}^N E_{\alpha} e^{-\frac{E_{\alpha}}{k_B T}}}{\sum_{\alpha=1}^N e^{-\frac{E_{\alpha}}{k_B T}}} \quad (2.53)$$

Where T is the temperature and k_B is the Boltzmann constant.

Now, the heat capacity can be calculated from the temperature derivative of the mean energy of the QD.

$$C_v(T, B, \omega_o) = \frac{\partial \langle E(T, B, \omega_o) \rangle}{\partial T} \quad (2.54)$$

We have computed numerical value of the heat capacity of the QD system for various ranges of the magnetic field ω_c , confining frequency ω_0 and temperature T . The obtained results are displayed in the next chapter.

Chapter Three

Result and Discussion

3.1 Quantum Dot Spectra

3.2 Heat Capacity

Chapter Three

Result and Discussion

3.1 Energy spectra

Our computed results for two interacting electrons in a quantum dot made from GaAs material ($m^* = 0.067 m_e, R^* = 5.825 meV$) are presented in this chapter.

In the Absence of the magnetic field, the states of the QD system are degenerate as shown in figure (3.1), while for finite strength of magnetic field, the degeneracy of the states are removed.

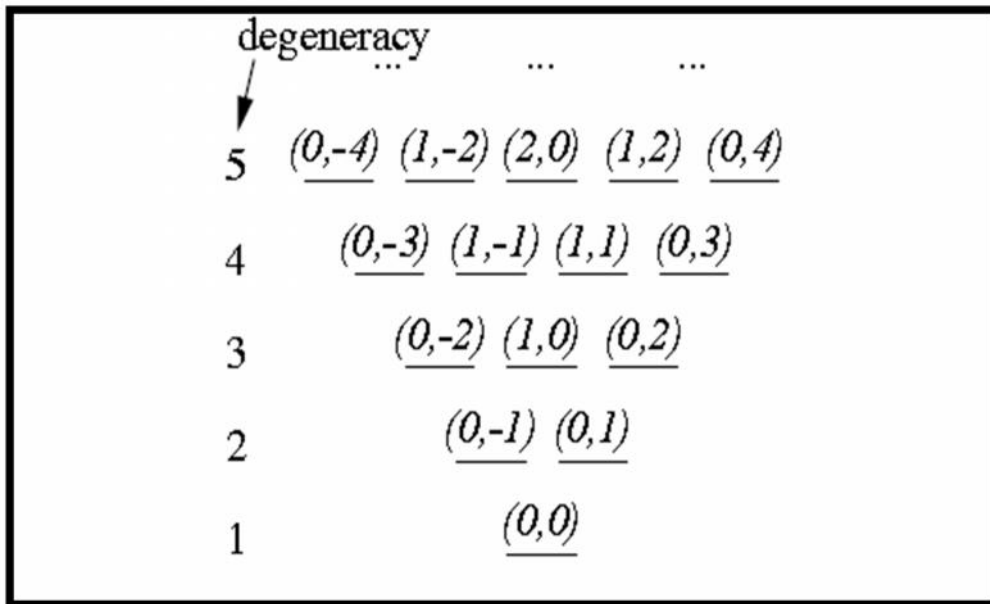


Figure (3.1) The energy spectra of Fock-Darwin states and the corresponding degeneracy.

We had plotted the computed energy results of this work against the strength of the magnetic field for $\omega_0 = \frac{2}{3} R^*$ for both non-interacting Figure (3.2) and interacting Figure (3.3) electrons. The non-interacting

graph shows that the ground state energy level (0,0) remains the lowest energy level as magnetic field increase while the interacting case shows clearly the transition in the angular momentum of the ground state of the QD system as the magnetic field increases. The origin of these transitions is due to the effect of coulomb interaction energy in the QD Hamiltonian. These transitions in the angular momentum of the QD system correspond to the (singlet-triplet) transitions are expected to manifest themselves as cusps in the heat capacity curve of the QD. The present results also show very good agreement compared with Dyblaski's result [27], where the authors had used the same variational wave function. In addition, we had displayed the energy result for interacting electrons in table 1, and one could clearly notice the transition of ground state angular momentum when the magnetic field strength increase.

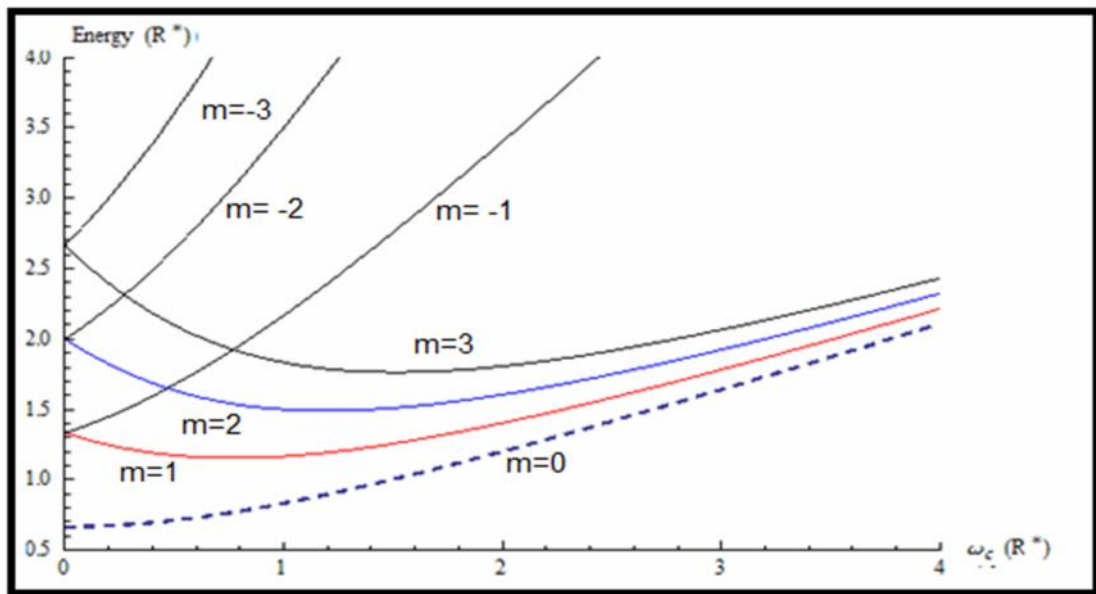


Figure (3.2) The dependence of the relative motion energy spectra on the magnetic field for two non-interacting electrons in a QD at confining frequency $\omega_o = \frac{2}{3} R^*$

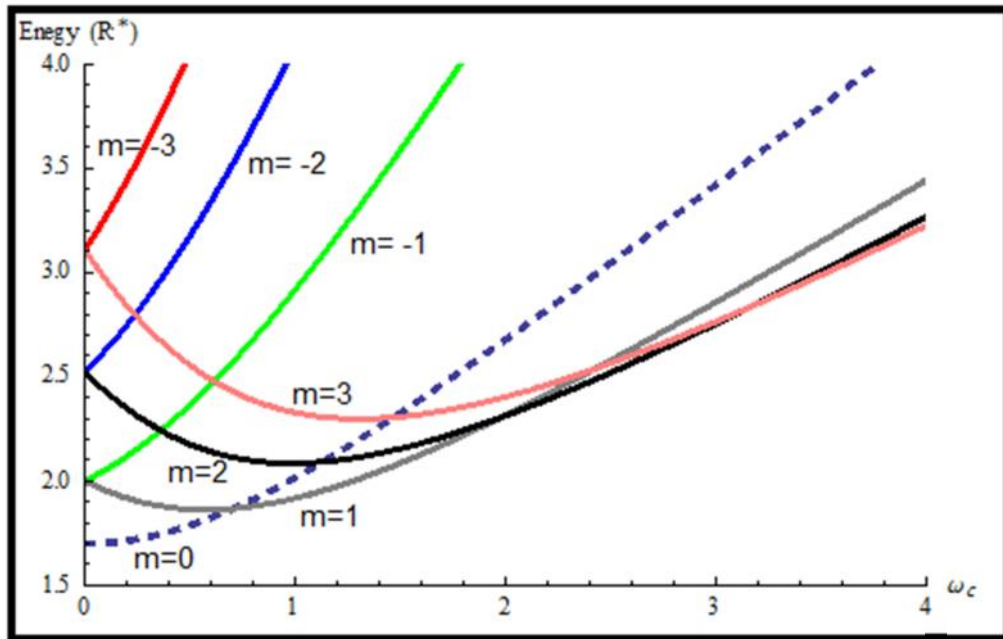


Figure (3.3) The computed relative motion energy spectra of two interacting electrons quantum dot against the strength of the magnetic field for $\omega_0 = \frac{2}{3}R^*$, and angular momentum $m_r = 0, \pm 1, \pm 2, \pm 3$.

Table (3.1) The relative motion energy spectra of the QD states ($m=0,1,2,\dots,8$) against the magnetic field for two interacting electrons for $\omega_o = \frac{2}{3} R^*$ (the underlined energy values show the angular momentum transitions of the ground state of the QD).

	<u>m</u>					
	0	1	2	3	4	5
0.	<u>1.69986</u>	2.	2.52194	3.10835	3.72268	4.3519
0.1	1.7035	1.95475	2.42832	2.96647	3.5326	4.11363
0.2	1.71434	1.91891	2.34733	2.8407	3.36218	3.89863
0.3	1.73217	1.89223	2.27866	2.73063	3.21093	3.70632
0.4	1.75667	1.8743	2.22179	2.6356	3.07806	3.53577
0.5	1.7874	1.86462	2.17605	2.55479	2.96258	3.38581
0.6	1.82387	1.86258	2.14066	2.48723	2.8633	3.25504
0.7	1.86555	1.86754	2.11479	2.43186	2.77896	3.14198
0.8	1.91192	<u>1.87885</u>	2.09759	2.38763	2.70826	3.04511
0.9	1.96243	1.89585	2.08821	2.35346	2.64992	2.96291
1.	2.01661	1.91795	2.08586	2.32835	2.60271	2.89393
1.1	2.07397	1.94455	2.08978	2.31135	2.56547	2.8368
1.2	2.13411	1.97515	2.09927	2.30157	2.53714	2.79028
1.3	2.19664	2.00926	2.1137	2.29823	2.51676	2.75322
1.4	2.26124	2.04646	2.13252	2.30061	2.50345	2.7246
1.5	2.32761	2.08637	2.15523	2.30808	2.49643	2.70348
1.6	2.39548	2.12867	2.18137	2.32005	2.49501	2.68905
1.7	2.46465	2.17307	2.21055	2.33605	2.49858	2.6806
1.8	2.53492	2.2193	2.24244	2.35561	2.50661	2.67748
1.9	2.60611	2.26715	2.27673	2.37837	2.51861	2.67912
2.	2.67808	2.31643	<u>2.31314</u>	2.40396	2.53417	2.68502
2.1	2.75072	2.36696	2.35146	2.4321	2.55291	2.69476
2.2	2.82391	2.41859	2.39147	2.46252	2.57451	2.70794
2.3	2.89755	2.4712	2.43299	2.49498	2.59869	2.72422
2.4	2.97157	2.52467	2.47587	2.52929	2.62518	2.74329
2.5	3.04591	2.5789	2.51997	2.56524	2.65377	2.7649
2.6	3.12049	2.63381	2.56515	2.6027	2.68426	2.7888
2.7	3.19527	2.68931	2.61132	2.64151	2.71646	2.81478
2.8	3.2702	2.74535	2.65837	2.68154	2.75023	2.84265
2.9	3.34525	2.80186	2.70623	2.72269	2.78541	2.87225
3.	3.42038	2.85879	2.7548	2.76485	2.8219	2.90343
3.1	3.49556	2.91609	2.80403	2.80793	2.85957	2.93605
3.2	3.57077	2.97372	2.85386	<u>2.85186</u>	2.89832	2.96999
3.3	3.64599	3.03164	2.90422	2.89655	2.93806	3.00515
3.4	3.72119	3.08983	2.95507	2.94195	2.97872	3.04143
3.5	3.79636	3.14825	3.00638	2.988	3.02022	3.07873
3.6	3.87149	3.20687	3.05809	3.03464	3.06249	3.11699
3.7	3.94656	3.26568	3.11017	3.08182	3.10548	3.15612
3.8	4.02157	3.32466	3.16259	3.12951	3.14912	3.19606
3.9	4.0965	3.38377	3.21532	3.17766	3.19337	3.23676

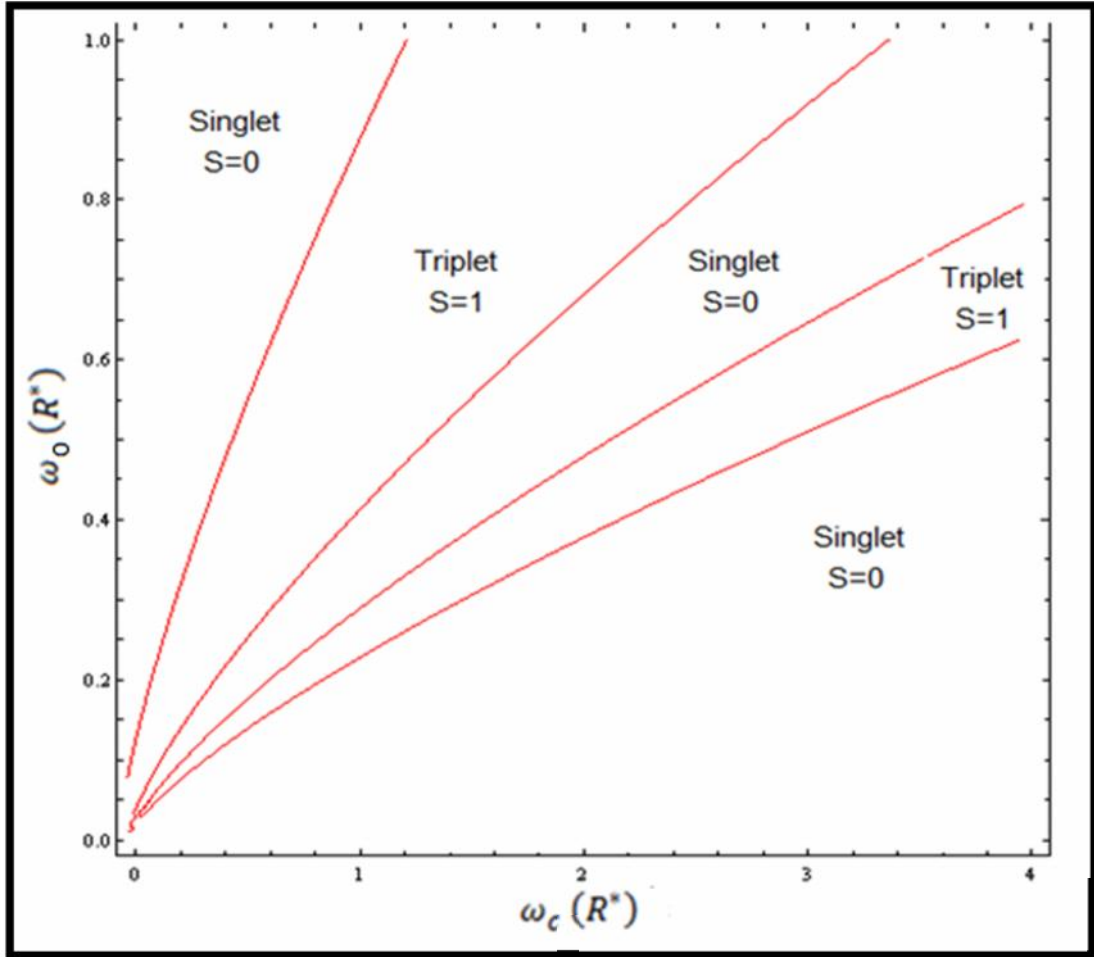
Magnetic field strength ω_c

Continue of the tablem

	3	4	5	6	7	8
4.	3.22624	3.23819	3.27816	3.3348	3.40228	3.47728
4.1	3.27522	3.28353	3.32021	3.37374	3.43826	3.51037
4.2	3.32456	3.32936	3.36286	3.41341	3.47507	3.54441
4.3	3.37424	3.37564	3.40607	3.45375	3.51266	3.57934
4.4	3.42423	<u>3.42235</u>	3.44981	3.49472	3.55098	3.6151
4.5	3.47452	3.46944	3.49404	3.53628	3.58998	3.65163
4.6	3.52507	3.5169	3.53873	3.57838	3.62962	3.68889
4.7	3.57588	3.56471	3.58385	3.621	3.66986	3.72684
4.8	3.62693	3.61283	3.62937	3.6641	3.71067	3.76543
4.9	3.67819	3.66125	3.67526	3.70766	3.752	3.80462
5.	3.72966	3.70995	3.72151	3.75164	3.79383	3.84438
5.1	3.78131	3.75892	3.7681	3.79602	3.83613	3.88467
5.2	3.83315	3.80813	3.81499	3.84078	3.87887	3.92547
5.3	3.88514	3.85757	3.86218	3.8859	3.92203	3.96675
5.4	3.9373	3.90723	3.90965	3.93135	3.96558	4.00848
5.5	3.9896	3.95709	3.95738	3.97712	4.0095	4.05063
5.6	4.04203	4.00715	<u>4.00536</u>	4.02319	4.05378	4.09319
5.7	4.0946	4.05739	4.05357	4.06954	4.09839	4.13613
5.8	4.14728	4.1078	4.10199	4.11617	4.14331	4.17943
5.9	4.20007	4.15836	4.15063	4.16304	4.18853	4.22308
6.	4.25297	4.20909	4.19946	4.21016	4.23404	4.26705
6.1	4.30596	4.25995	4.24848	4.2575	4.27982	4.31133
6.2	4.35905	4.31095	4.29768	4.30506	4.32585	4.35591
6.3	4.41222	4.36207	4.34704	4.35283	4.37212	4.40077
6.4	4.46548	4.41332	4.39657	4.40079	4.41863	4.44589
6.5	4.51881	4.46468	4.44624	4.44893	4.46535	4.49127
6.6	4.57221	4.51615	4.49605	4.49726	4.51229	4.53689
6.7	4.62568	4.56772	4.54601	<u>4.54575</u>	4.55943	4.58274
6.8	4.67921	4.61939	4.59609	4.5944	4.60675	4.62881
6.9	4.7328	4.67115	4.64629	4.64321	4.65426	4.6751
7.	4.78645	4.723	4.69661	4.69216	4.70194	4.72158
7.1	4.84015	4.77493	4.74704	4.74125	4.74979	4.76826
7.2	4.89389	4.82694	4.79758	4.79047	4.7978	4.81512
7.3	4.94769	4.87902	4.84821	4.83981	4.84595	4.86215
7.4	5.00153	4.93118	4.89895	4.88928	4.89426	4.90935
7.5	5.0554	4.9834	4.94977	4.93887	4.9427	4.95672
7.6	5.10932	5.03568	5.00069	4.98856	4.99127	5.00424
7.7	5.16327	5.08803	5.05168	5.03836	5.03997	5.05191
7.8	5.21726	5.14043	5.10276	5.08826	5.08879	5.09971
7.9	5.27127	5.19289	5.15391	5.13826	<u>5.13773</u>	5.14766

Magnetic field strength ωc

The angular momentum dependence on confinement frequency is displayed in figure (3.4)



Figure(3.4) The singlet-triplet phase diagram of the QD. Confining frequency ω_o against the strength of the magnetic field ω_c

To deeply understand this transition we had plotted the singlet-triplet gap for specific confinement frequency $\omega_o = \frac{2}{3}$, which clearly shows that the ground state angular momentum changed from $l = 0$ to $l = 1$ at certain magnetic field values which depend on the confinement frequency figure(3.5).

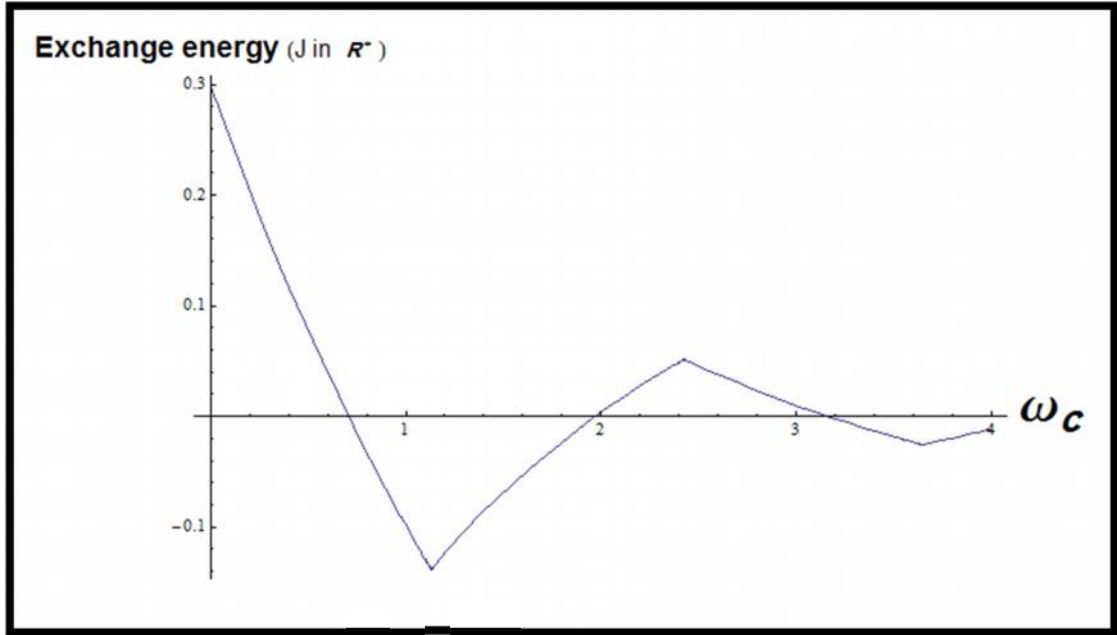


Figure (3.5) The exchange energy of the two interacting electrons in a QD against the magnetic field strength for $\omega_o = \frac{2}{3} R^*$

3.2 Heat capacity

In Figure (3.6) we had shown the behavior of the heat capacity C_v against the temperature for different values of the confining frequency ω_o , while keeping ω_c unchanged. For particular confining frequency ω_o , the heat capacity curve shows a peak value at low temperature, while at high temperature degrees the heat capacity saturates. This behavior for the heat capacity is in agreement with the results of Refs.[21, 22, 28, 29]. As the confining frequency increases, the peak of the heat capacity shifts to a higher temperature, numerical values of the heat capacity against the temperature are shown in Table (2).

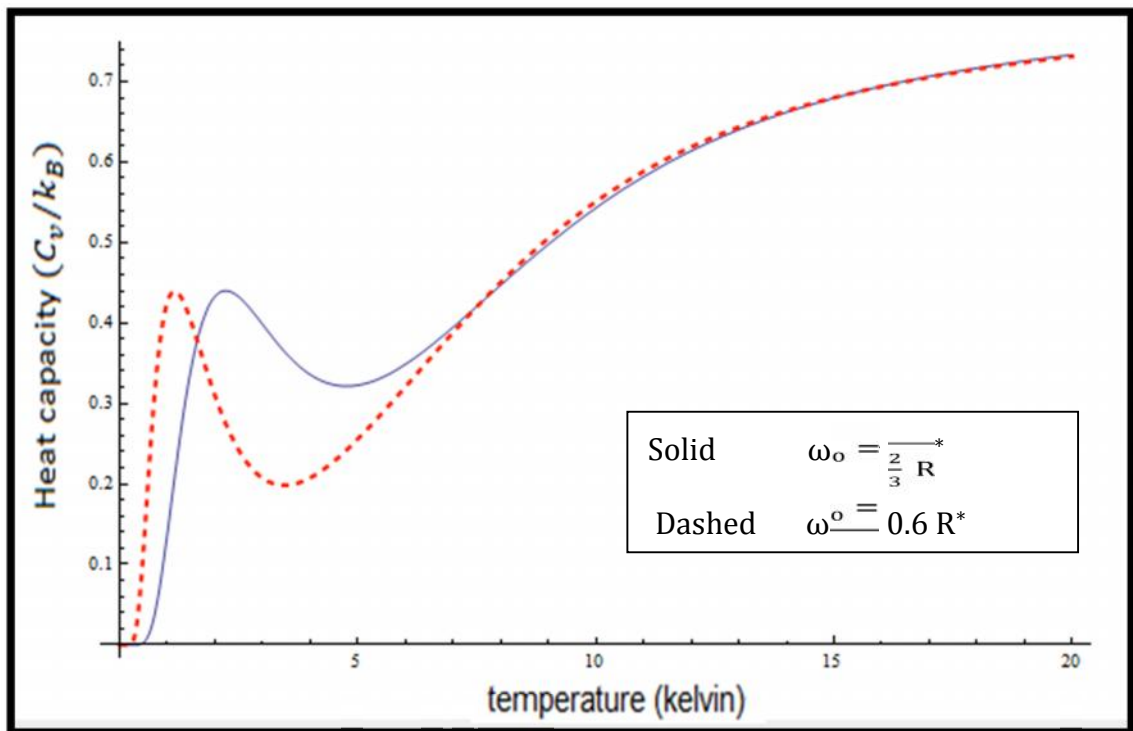


Figure (3.6) The dependence of the heat capacity on the temperature for fixed value of magnetic field $\omega_c = 0.5 R^*$ and various confinement frequencies: $\omega_o = \frac{2}{3} R^*$ Solid , $\omega_o = 0.6 R^*$ Dashed.

In Figure (3.7) we had shown the dependence of the heat capacity on the magnetic field strength for fixed values of the confining frequency and temperature. The heat capacity shows a peak structure which is a result of the transition in the angular momentum of the ground state energy as shown and discussed previously in Figure (3.3). For example, the first peak corresponds to the transition in the angular momentum of the ground state from $m_r = 0$ to $m_r = 1$.

Table (3.2) The heat capacity of two interacting electrons QD against the temperature for $\omega_o = \frac{2}{3} R^*$ and $\omega_c = 0.5 R^*$

T	$\frac{C_V}{C_V}$	T	$\frac{C_V}{C_V}$	T	$\frac{C_V}{C_V}$
0.	0.	4.	0.335805	8.	0.447141
0.1	0.	4.1	0.332201	8.1	0.45238
0.2	0.	4.2	0.329137	8.2	0.457594
0.3	6.58844×10^{-6}	4.3	0.326607	8.3	0.462777
0.4	0.000307524	4.4	0.324599	8.4	0.467926
0.5	0.00278886	4.5	0.323101	8.5	0.473036
0.6	0.0113384	4.6	0.322095	8.6	0.478103
0.7	0.0294182	4.7	0.321565	8.7	0.483125
0.8	0.0579614	4.8	0.32149	8.8	0.488098
0.9	0.0953708	4.9	0.321852	8.9	0.493019
1.	0.138626	5.	0.322628	9.	0.497886
1.1	0.184392	5.1	0.323799	9.1	0.502697
1.2	0.229715	5.2	0.325342	9.2	0.507448
1.3	0.272334	5.3	0.327236	9.3	0.51214
1.4	0.310731	5.4	0.329461	9.4	0.51677
1.5	0.34404	5.5	0.331996	9.5	0.521336
1.6	0.371918	5.6	0.33482	9.6	0.525838
1.7	0.394398	5.7	0.337914	9.7	0.530274
1.8	0.411768	5.8	0.341258	9.8	0.534645
1.9	0.424471	5.9	0.344833	9.9	0.538948
2.	0.433031	6.	0.348621	10.	0.543184
2.1	0.438	6.1	0.352606	10.1	0.547353
2.2	0.439923	6.2	0.356769	10.2	0.551453
2.3	0.439318	6.3	0.361095	10.3	0.555486
2.4	0.43666	6.4	0.365569	10.4	0.55945
2.5	0.432375	6.5	0.370176	10.5	0.563346
2.6	0.426842	6.6	0.374901	10.6	0.567175
2.7	0.420389	6.7	0.379731	10.7	0.570936
2.8	0.413301	6.8	0.384654	10.8	0.57463
2.9	0.405816	6.9	0.389657	10.9	0.578258
3.	0.398139	7.	0.394729	11.	0.581819
3.1	0.390437	7.1	0.399859	11.1	0.585315
3.2	0.38285	7.2	0.405037	11.2	0.588745
3.3	0.37549	7.3	0.410254	11.3	0.592112
3.4	0.368449	7.4	0.415499	11.4	0.595415
3.5	0.361795	7.5	0.420765	11.5	0.598655
3.6	0.355584	7.6	0.426044	11.6	0.601833
3.7	0.349856	7.7	0.431327	11.7	0.60495
3.8	0.34464	7.8	0.436609	11.8	0.608006
3.9	0.339953	7.9	0.441882	11.9	0.611003

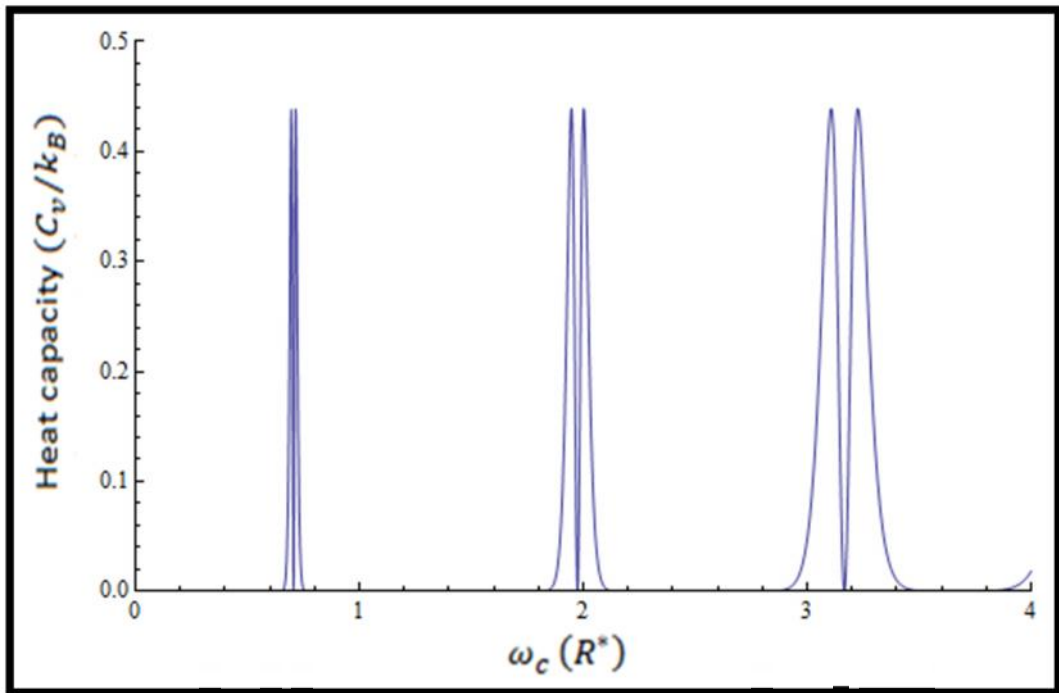


Figure (3.7) The heat capacity as function of magnetic field strength for fixed value of temperature ($T = 0.1$ K) and confinement frequency $\omega_0 = \frac{2}{3} R^*$.

Chapter Four

Conclusion and Future Work

Chapter Four

Conclusion and future work

In conclusion, we had applied the variational method to solve the Hamiltonian for interacting electrons confined parabolically in a quantum dot subjected to a magnetic field. We had used the one variation parameter wave function to get the minimized energy expression. In addition, we had shown the angular momentum transitions in the ground state of GaAs/AlGaAs quantum dot spectra. These level crossings which result of Coulomb interaction cause oscillations in the heat capacity curve of the quantum dot. In addition we had investigated the dependence of the heat capacity of the QD on the system parameters ω_0 , ω_c , and T. The results of both, the eigenenergies and the heat capacity, calculated by variational method show very good agreement comparable with other recent works.

In this work we had taken the heat capacity as a thermal property of the QD system, however another thermodynamic and magnetic quantities like magnetization and magnetic susceptibility can be considered in the future. We expect that the angular momentum transition of the ground state will affect significantly the magnetic properties of the QD. In addition the electronic and magnetic properties of few electrons QD are important issues to be studied.

References

- 1) R. C. Ashoori, H. L. Stormer, J. S. Weiner, L. N. Pfeiffer, K. W. Baldwin, and K. W. West. ***N*-electron ground state energies of a quantum dot in magnetic field**, Phys. Rev. Lett. **71**, 613 (1993).
- 2) R. C. Ashoori. **Electrons in artificial atoms**, Nature **379**, 413 (1996)
- 3) Orion Ciftja. **Understanding electronic systems in semiconductor quantum dots**, Phys. Scr. **88**, 058302 (2013).
- 4) M. A. Kastner, **The single-electron transistor**, Rev. Mod. Phys. **64**, 849 (1992).
- 5) D. Loss and D. P. Divincenzo. **Quantum computation with quantum dots**, Phys. Rev. A **57**, 120 (1998).
- 6) G. Burkard, D. Loss and D. P. Divincenzo. **Coupled quantum dots as quantum gates**, Phys. Rev. **B 59**, 2070 (1999).
- 7) P. A. Maksym and Tapash Chakraborty. **Quantum dots in a magnetic field: Role of electron-electron interactions**, Phys. Rev. Lett. **65** , 108 (1990).
- 8) M. Wagner, U. Merkt and V. Chaplik. **Spin-singlet–spin-triplet oscillations in quantum dots**, Phys. Rev. **B 45**, 1951 (1992).

- 9) S. Tarucha, D. G. Austing, T. Honda, R. J. van der Hage, and L. P. Kouwenhoven. **Shell Filling and Spin Effects in a Few Electron Quantum Dot**, Phys. Rev. Lett. **77**, 3613 (1996).
- 10) M. Taut. **Two electrons in a homogeneous magnetic field: particular analytical solutions**, J. Phys. A: Math. Gen. **27**, 1045 (1994).
- 11) Orion Ciftja and Anil Kumar. **Perturbation, diagonalization, and variational theory Ground state of two-dimensional quantum-dot helium in zero magnetic field**, Phys. Rev. **B 70**, 205326 (2004).
- 12) Orion Ciftja and M. Golam Faruk. **Two-dimensional quantum-dot helium in a magnetic field: Variational theory**, Phys. Rev. **B 72**, 205334 (2005).
- 13) B. S. Kandemir. **Variational study of two-electron quantum dots**, Phys. Rev. **B 72**, 165350 (2005).
- 14) B. S. Kandemir. **Two interacting electrons in a uniform magnetic field and a parabolic potential: The general closed-form solution**, J. Math. Phys. **46**, 032110 (2005).
- 15) M. Elsaid. **Spectroscopic structure of two interacting electrons in a quantum dot by the shifted $1/N$ expansion method**, Phys. Rev. **B 61**, 13026 (2000).

- 16) M. Elsaid. **Two-electron quantum dots in a magnetic field**, Semiconductor Sci. Technol. **10**, 1310 (1995).
- 17) M. Elsaid. **The energy level ordering in two-electron quantum dot spectra**, Superlattices and Microstructures, **23**, 1237 (1998).
- 18) M. Elsaid, M. Al-Nafaa and S. Zugail. **Spin Singlet-Triplet Energy Splitting in the Ground State of a Quantum Dot with a Magnetic Field: Effect of Dimensionality**, J.Computational and Theoretical Nanoscience, **5**, 677 (2008).
- 19) M. Elsaid. **The Spectral Properties of two Interacting Electrons in a Quantum Dot**, Turk. J. Phys, **26**, 331 (2002).
- 20) Jean. Jacques S. De Groote and J. E. M. Hornos and A.V. Chaplik. **Thermodynamic properties of quantum dots in a magnetic field**, Phys. Rev. **B 46**, 12773 (1992).
- 21) Nag T. T. Nguyen and F. M Peeters. **Magnetic field dependence of the many-electron states in a magnetic quantum dot: The ferromagnetic-antiferromagnetic transition**, Phys. Rev. **B 78**, 045321 (2008).
- 22) B. Boyacioglu and A. Chatterjee. **Heat capacity and entropy of a GaAs quantum dot with Gaussian confinement**, J. Appl. Phys. **112**, 083514 (2012).

- 23) M. Helle, A. Harju and R.M. Nieminen. **Two-electron lateral quantum-dot molecules in a magnetic field**, Phys. Rev. B **72**, 205329 (2005).
- 24) V. Fock. **Bemerkung zur Quantelung des harmonischen Oszillators im Magnetfeld**, Z. Phys. **47**, 446 (1928).
- 25) C. G. Darwin. **The Diamagnetism of the Free Electron**, Math. Proc. Cambridge Phill. Soc. **27**, 86 (1930).
- 26) W. Dybalski and P. Hawrylak. **Two electrons in a strongly coupled double quantum dot: From an artificial helium atom to a hydrogen molecule**, Phys. Rev. B **72**, 205432 (2005).
- 27) S. A. Mikhailov. **Quantum-dot lithium in zero magnetic field: Electronic properties, thermodynamics, and Fermi liquid–Wigner solid crossover in the ground state**, Phys. Rev. B **65**, 115312 (2002).
- 28) H. M Muller and S. E. Koonin. **Phase transitions in quantum dots**, Phys. Rev. B **54**, 14532 (1996).

جامعة النجاح الوطنية
كلية الدراسات العليا

السعة الحرارية لنقطة كمية تحتوي إلكترونين في مجال مغناطيسي خارجي "بطريقة المتغيرات"

إعداد

أيهم أنور شاعر

إشراف

أ. د. محمد السعيد

د. موسى الحسن

قدمت هذه الأطروحة استكمالاً لمتطلبات الحصول على درجة الماجستير في الفيزياء
في كلية الدراسات العليا في جامعة النجاح الوطنية - نابلس.

2015

السعة الحرارية لنقطة كمية تحتوي إلكترونيين
في مجال مغناطيسي خارجي "بطريقة المتغيرات"

إعداد

أيهم أنور شاعر

إشراف

أ. د. محمد السعيد

د. موسى الحسن

المخلص

تم حساب السعة الحرارية لزوج من الإلكترونات المتشادة والمحصورة في نقطة كمية والموضوعة أيضا في مجال مغناطيسي وذلك عن طريق حل دالة هاملتون باستخدام طريقة المتغيرات. ولقد قمنا بدراسة اعتماد السعة الحرارية على كل من درجة الحرارة والمجال المغناطيسي بالإضافة لتردد الحصر. كما وضحت الدراسة الانتقال الأحادي-الثلاثي للزخم الزاوي للمستوى الأرضي والقفزات في منحنى السعة الحرارية الناتجة عنه. وأظهرت المقارنات توافق كبير بين نتائجنا مع نتائج أعمال أخرى منشورة.